Role of the Ancillary Ligand *N*,*N*-Dimethylaminoethanol in the Sensitization of Eu^{III} and Tb^{III} Luminescence in Dimeric β-Diketonates

Svetlana V. Eliseeva,*,† Oxana V. Kotova,† Frédéric Gumy,‡ Sergey N. Semenov,†,⊥ Vadim G. Kessler,§ Leonid S. Lepnev,|| Jean-Claude G. Bünzli,‡ and Natalia P. Kuzmina†

Department of Chemistry, Department of Materials Sciences, Lomonosov Moscow State University, Leninskie Gory 1-3, 119991 Moscow, Russia, Laboratory of Lanthanide Supramolecular Chemistry, École Polytechnique Fédérale de Lausanne (EPFL), BCH 1405, 1015 Lausanne, Switzerland, Department of Chemistry, Swedish University of Agricultural Sciences, P.O. Box 7015, 75007 Uppsala, Sweden, and Vavilov Luminescence Laboratory, Lebedev Physical Institute of Russian Academy of Sciences, Leninsky Prospect 53, 119991 Moscow, Russia

Received: November 29, 2007; In Final Form: January 29, 2008

Two types of dimeric complexes $[Ln_2(hfa)_6(\mu_2\text{-}O(CH_2)_2NHMe_2)_2]$ and $[Ln(thd)_2(\mu_2,\eta^2\text{-}O(CH_2)_2NMe_2)]_2$ (Ln = Y^{III}, Eu^{III}, Gd^{III}, Tb^{III}, Tm^{III}, Lu^{III}; hfa^- = hexafluoroacetylacetonato, thd^- = dipivaloylmethanato) are obtained by reacting $[Ln(hfa)_3(H_2O)_2]$ and $[Ln(thd)_3]$, respectively, with *N*,*N*-dimethylaminoethanol in toluene and are fully characterized. X-ray single crystal analysis performed for the Tb^{III} compounds confirms their dimeric structure. The coordination mode of *N*,*N*-dimethylaminoethanol depends on the nature of the β-diketonate. In $[Tb_2(hfa)_6(\mu_2\text{-}O(CH_2)_2NHMe_2)_2]$, eight-coordinate Tb^{III} ions adopt distorted square antiprismatic coordination environments and are O-bridged by two zwitterionic *N*,*N*-dimethylaminoethanol ligands with a Tb1···Tb2 separation of 3.684(1) Å. In $[Tb(thd)_2(\mu_2,\eta^2\text{-}O(CH_2)_2NMe_2)]_2$, the *N*,*N*-dimethylaminoethanol acts as chelating-bridging O,N-donor anion and the Tb^{III} ions are seven-coordinate; the Tb1···Tb1A separation amounts to 3.735(2) Å within centrosymmetric dimers. The dimeric complexes are thermally stable up to 180 °C, as shown by thermogravimetric analysis, and their volatility is sufficient for quantitative sublimation under reduced pressure. The Eu^{III} and Tb^{III} dimers display metal-centered luminescence, particularly $[Eu_2(hfa)_6(O(CH_2)_2NHMe_2)_2]$ (quantum yield Q^L_{Ln} = 58%) and $[Tb(thd)_2(O(CH_2)_2NMe_2)]_2$ (32%). Consideration of energy migration paths within the dimers, based on the study of both pure and Eu^{III}- or Tb^{III}-doped (0.01−0.1 mol %) Lu^{III} analogues, leads to the conclusion that both the β-diketone and *N*,*N*-dimethylaminoethanol ligands contribute significantly to the sensitization process of the Eu^{III} luminescence. The ancillary ligand increases considerably the luminescence of $[Eu_2(hfa)_6(O(CH_2)_2NHMe_2)_2]$, compared to $[Ln(hfa)_3(H_2O)_2]$, through the formation of intra-ligand states while it is detrimental to Tb^{III} luminescence in both β-diketonates. Thin films of the most luminescent compound $[Eu_2(hfa)_6(O(CH_2)_2NHMe_2)_2]$ obtained by vacuum sublimation display photophysical properties analogous to those of the solid-state sample, thus opening perspectives for applications in electroluminescent devices.

Introduction

Lanthanide(III) β-diketonates are among the most thoroughly investigated classes of coordination compounds. The considerable attention they have been attracting until now stems from both their easy synthesis and the variety of practical applications in which they can be involved.[1] In neutral lanthanide tris(β-diketonates), the central ions are bound to six oxygen atoms and thus coordinatively unsaturated. This results in the possibility of binding one or more ancillary ligands to achieve the usual coordination numbers observed in most lanthanide complexes (8−10) and to implement a desired functionality. The latter property is widely used in NMR shift reagents,[2] catalysis,[3] and sensing/probing devices.[4] Such applications require a precise tuning of the coordination properties of the lanthanide ions and an adequate choice of both primary and ancillary ligands to control the competitive coordination of substrates, solvents, and other molecules. Aminoalcohols behave either as anionic or neutral (respectively zwitterionic) ligands and adopt a variety of binding modes due to the presence of two donor atoms, nitrogen and oxygen, which are easily accessible for coordination. For instance, they can act as monodentate ligands binding metal ions through either oxygen, similarly to alcohols and alkoxides,[5] or nitrogen, such as amines, as shown in [Cu(hfa)(L)] where L is deprotonated triethanolamine or *N*,*N*-dimethylethanolamine.[6] Alternatively, they can bind in a bidentate fashion through both oxygen and nitrogen atoms, adopting terminal/bridging, chelating, or bridging/chelating modes.[7−10] Taking into account the pronounced hard Lewis acid character of trivalent lanthanide ions,[11] it is anticipated that coordination to these ions will essentially be achieved through oxygen binding.

Recently, Tsukube et al.[12] have reported the use of lanthanide tris(β-diketonates) as chirality sensing agents for aminoalcohols. For instance, fluorinated lanthanide β-diketonates form 1:1

* To whom correspondence should be addressed. E-mail: eliseeva@inorg.chem.msu.ru. Phone: +7-495-939-3836. Fax: +7-495-939-0998.
† Lomonosov Moscow State University.
‡ École Polytechnique Fédérale de Lausanne (EPFL).
§ Swedish University of Agricultural Sciences.
|| Lebedev Physical Institute of Russian Academy of Sciences.
⊥ Present address: University of Zürich, Institute of Inorganic Chemistry, Winterthurerstrasse 190, CH 8057, Switzerland.

10.1021/jp711305u CCC: $40.75
Published on Web 03/22/2008

highly coordinated complexes with aminoalcohols in MeOH/CH_2Cl_2 solution in which the aminoalcohol acts as ancillary bidentate neutral ligand. The resulting complexes exhibit largely enhanced luminescence and intense induced circular dichroism signals. The latter depend on the structure and chirality of the bound aminoalcohol. However, only one crystal structure of such a mixed complex, namely $[Pr_2(hfa)_4(bdmap)_2(H_2O)_2(thf)_2]$ (bdmap = 1,3-bis(dimethylamino)-2-propoxide, thf = tetrahydrofuran), is described.[9]

In this work, we investigate the reaction of *N*,*N*-dimethylaminoethanol with fluorinated (hexafluoroacetyl-acetonato, hfa^-) and bulky (dipivaloylmethanato, thd^-) lanthanide β-di-ketonates, which turned to yield dimeric species. The two series of complexes, namely $[Ln_2(hfa)_6(O(CH_2)_2NHMe_2)_2]$ and $[Ln(thd)_2(O(CH_2)_2NMe_2)]_2$ (Ln = Y^{III}, Eu^{III}, Gd^{III}, Tb^{III}, Tm^{III}, Lu^{III}), are structurally characterized, and their thermal and photophysical properties are investigated. To access more information about energy-transfer processes in the reported Eu^{III} and Tb^{III} compounds, the photophysical properties of both pure and Eu^{III}- or Tb^{III}-doped Lu^{III} complexes are also studied. Finally, to evaluate the potential of the new dimeric complex $[Eu_2(hfa)_6(O(CH_2)_2NHMe_2)_2]$ as an emitting layer in electroluminescent devices, thin films of this derivative are produced by vacuum sublimation, and their emissive properties are compared with those of the corresponding solid-state sample.

Experimental Section

Reagents and Physical Methods. Commercially available starting reagents Hhfa (Merck), Hthd (Aldrich), and *N*,*N*-dimethylaminoethanol (Aldrich) were of analytical grade and used as received. Lanthanide nitrate hydrates $Ln(NO_3)_3{\cdot}xH_2O$ were obtained by treating the respective lanthanide oxides Ln_2O_3 (99.998%) or Tb_4O_7 (99.998%) with concentrated nitric acid, followed by evaporation of excess acid. $[Ln(hfa)_3(H_2O)_2]$ and $[Ln(thd)_3(H_2O)_2]$ were synthesized according to procedures described in ref 13 and 14, respectively. $[Ln(thd)_3]$ were obtained by sublimation of the corresponding hydrated complexes at 180−200 °C under a pressure of 10^{-2} Torr.

Elemental analyses (C, H, N) were performed by the Microanalytical Service of the Center for Drug Chemistry (Moscow, Russia). IR spectra were recorded in Nujol mull or hexachlorobutadiene between KBr plates in the 4000−400 cm^{-1} range using a Perkin-Elmer 1600 FT-IR spectrometer. LDI-TOF mass spectra were run on an Autoflex II (Bruker Daltonics, Germany) using the electron-impact positive mode (accelerating voltage 19 kV) and a nitrogen laser (337 nm, impulse duration 1 ns). Thermogravimetric analysis was performed on a Q-1500 thermal analyzer in nitrogen atmosphere at a heating rate of 5 °C·min^{-1}. Isothermal dynamic sublimation experiments were run with samples (∼100 mg) placed into glass test tubes for periods of about 30 min at 220−240 °C and a pressure of 10^{-2} Torr. Weight loss was equal to ∼95−100%.

Syntheses. *$[Ln_2(hfa)_6(\mu_2\text{-}O(CH_2)_2NHMe_2)_2]$.* To a suspension of $[Ln(hfa)_3(H_2O)_2]$ (0.40 mmol) in 5 mL of toluene, *N*,*N*-dimethylaminoethanol (0.04 mL, 0.40 mmol) was added dropwise under stirring. The resulting transparent solution was allowed to stay for 2−3 days at 258 K. The crystalline fraction was isolated by decantation and dried in vacuum. Yield: 85−90%.

$C_{38}H_{28}F_{36}N_2O_{14}Y_2$ (1598.39): calcd C 28.55, H 1.77, N 1.75; found C 28.76, H 1.59, N 1.75%. IR data: $\tilde{\nu}$ = 3392 br w; 3306 w; 3114 br m; 2974 w; 2906 w; 1666 br s; 1656 br s; 1600 m; 1562 s; 1536 s; 1518 s; 1502 m; 1478 m; 1470 m; 1464 m; 1440 m; 1402 m; 1390 m; 1350 m; 1322 m; 1260 br s; 1210 br s; 1146 br s; 1098 s; 1078 s; 1006 w; 986 w; 952 w; 920 w; 886 w; 798 s; 768 w; 742 m; 722 w; 662 s; 588 m; 528 w; 466 w cm^{-1}.

$C_{38}H_{28}F_{36}N_2O_{14}Eu_2$ (1724.52): calcd C 26.47, H 1.64, N 1.62; found C 26.35, H 1.81, N 1.82%. IR data: $\tilde{\nu}$ = 3396 br w; 3306 w; 3098 m; 2902 w; 1662 br s; 1654 br s; 1606 m; 1560 s; 1532 s; 1510 s; 1476 s; 1460 s; 1438 m; 1424 m; 1390 m; 1348 m; 1322 m; 1256 br s; 1206 br s; 1142 br s; 1100 s; 1078 s; 1068 m; 1008 w; 984 w; 950 w; 922 w; 884 w; 838 w; 798 s; 766 w; 758 w; 742 m; 722 w; 662 s; 586 s; 528 w; 462 w cm^{-1}. LDI-TOF MS (EI^+): 519, $[Eu(CF_3COCHCO)_2(O(CH_2)_2NHMe_2) + 2H^+]^+$ (7%); 608, $[Eu(CF_3COCHCO)_2(O(CH_2)_2NHMe_2)_2 + 2H^+]^+$ (7%); 959, $[Eu_2(hfa)(CF_3COCHCO)_2(O(CH_2)_2NHMe_2)_2 - 3CH_3 + 2F + H^+]^+$ (90%); 1053, $[Eu_2(hfa)_2(CF_3COCHCO)(O(CH_2)_2NHMe_2)_2 + F)]^+$ (100%); 1148, $[Eu_2(hfa)_2(CF_3COCHCO)_2(O(CH_2)_2NHMe_2)_2 - 3CH_3 + F]^+$ (80%); 1243, $[Eu_2(hfa)_3(CF_3COCHCO)(O(CH_2)_2NHMe_2)_2 + 2H^+]^+$ (45%); 1429, $[Eu_2(hfa)_4(CF_3COCHCO)(O(CH_2)_2NHMe_2)_2 - F]^+$ (7%); 1524, $[Eu_3(hfa)_4(CF_3COCHCO)(O(CH_2)_2NHMe_2)_2 - 3CH_3 - F + 3H^+]^+$ (15%).

$C_{38}H_{28}F_{36}N_2O_{14}Gd_2$ (1735.09): calcd C 26.31, H 1.63, N 1.61; found C 26.30, H 1.75, N 1.74%. IR data: $\tilde{\nu}$ = 3396 br w; 3306 w; 3098 m; 2903 w; 1662 br s; 1654 br s; 1604 m; 1560 s; 1534 s; 1510 s; 1475 s; 1460 s; 1438 m; 1424 m; 1402 w; 1390 m; 1348 m; 1322 w; 1256 br s; 1206 br s; 1142 br s; 1100 s; 1078 s; 1068 m; 1008 m; 984 m; 950 w; 922 w; 886 w; 838 w; 798 s; 766 w; 758 w; 742 m; 722 w; 662 s; 586 s; 528 w; 462 w cm^{-1}.

$C_{38}H_{28}F_{36}N_2O_{14}Tb_2$ (1738.44): calcd C 26.25, H 1.62, N 1.61; found C 26.36, H 1.50, N 1.73%. IR data: $\tilde{\nu}$ = 3396 br w; 3304 w; 3094 m; 2904 w; 1664 br s; 1654 br s; 1604 m; 1560 s; 1535 s; 1512 s; 1474 s; 1460 s; 1438 w; 1424 w; 1400 w; 1392 w; 1348 m; 1322 w; 1256 br s; 1206 br s; 1142 br s; 1100 s; 1080 s; 1068 s; 1008 m; 986 m; 950 w; 922 w; 886 w; 838 w; 798 s; 766 w; 758 w; 742 m; 722 w; 662 s; 586 s; 528 w; 462 w cm^{-1}.

$C_{38}H_{28}F_{36}N_2O_{14}Tm_2$ (1758.46): calcd C 25.96, H 1.60, N 1.59; found C 25.96, H 1.58, N 1.62%. IR data: $\tilde{\nu}$ = 3392 br w; 3306 w; 3108 m; 2906 w; 1666 br s; 1656 br s; 1612 m; 1600 m; 1560 s; 1536 s; 1518 s; 1472 s; 1464 s; 1438 m; 1422 m; 1400 m; 1388 m; 1350 m; 1324 m; 1260 br s; 1210 br s; 1146 br s; 1100 m; 1080 m; 1068 m; 1008 w; 988 w; 952 w; 922 w; 886 w; 840 w; 798 m; 768 w; 742 w; 722 w; 662 s; 588 m; 528 w; 464 w cm^{-1}.

$C_{38}H_{28}F_{36}N_2O_{14}Lu_2$ (1770.51): calcd C 25.78, H 1.59, N 1.58; found C 25.61, H 1.58, N 1.58%. IR data: $\tilde{\nu}$ = 3410 br w; 3306 w; 3114 m; 3118 m; 2916 w; 1660 br s; 1604 m; 1560 s; 1536 s; 1508 s; 1474 s; 1464 s; 1438 m; 1422 m; 1400 m; 1388 m; 1350 m; 1324 m; 1260 br s; 1210 br s; 1144 br s; 1100 s; 1082 s; 1068 m; 996 w; 988 w; 952 w; 922 w; 888 w; 848 w; 800 s; 768 m; 742 m; 724 m; 662 s; 588 m; 528 w; 466 w cm^{-1}.

$[Ln(thd)_2(\mu_2,\eta^2\text{-}O(CH_2)_2NMe_2)]_2$. *N*,*N*-Dimethylaminoethanol (0.04 mL, 0.40 mmol) was added dropwise and under stirring to a suspension of $[Ln(thd)_3]$ (0.40 mmol) in 5 mL of toluene. The mixture first became transparent, and then a polycrystalline precipitate appeared. The solid was isolated by filtration or decantation. An additional portion was obtained by storing the mother liquor at 258 K. The obtained products were dried in vacuum. Overall yield: 85−90%.

$C_{52}H_{96}N_2O_{10}Y_2$ (1087.14): calcd C 57.45, H 8.90, N 2.58; found C 57.60, H 8.98, N 2.64%. IR data: $\tilde{\nu}$ = 2978 s; 2956 s; 2924 s; 2898 s; 2862 s; 2834 s; 2790 m; 1594 s; 1574 s; 1548

TABLE 1: Crystallographic Data and Some Details of Data Collection and Structures Refinement for the Tb^{III} Complexes with *N,N*-dimethylaminoethanol

compound	$[Tb_2(hfa)_6(O(CH_2)_2NHMe_2)_2]\cdot C_7H_8$	$[Tb(thd)_2(O(CH_2)_2NMe_2)]_2$
formula unit	$C_{45}H_{36}F_{36}N_2O_{14}Tb_2$	$C_{52}H_{96}N_2O_{10}Tb_2$
molecular weight	1830.60	1227.15
crystal system	monoclinic	monoclinic
space group	$P2_1/n$ (No. 14)	$P2_1/c$ (No. 14)
a, Å	20.334(5)	12.817(6)
b, Å	13.796(3)	16.192(1)
c, Å	23.228(4)	14.550(1)
α, °	90	90
β, °	95.03(4)	91.77(5)
γ, °	90	90
volume, Å^3	6491(2)	3018(4)
Z	8	2
$\rho_{calc.}$, g·cm^{-3}	1.873	1.350
T, K	295(2)	295(2)
crystal size, mm	0.35 × 0.25 × 0.20	0.45 × 0.40 × 0.35
linear absorption coefficient μ, cm^{-1}	23.2	23.7
θ range for data, °	1.3 − 23.0	1.9 − 28.4
total/observed [$I > 2\sigma(I)$] reflections	9008/5218	6878/4102
parameters refined/ restraints	907/174	298/0
R_1, ωR_2	0.059, 0.104	0.040, 0.072

s; 1538 s; 1504 s; 1490 s; 1480 s; 1450 s; 1426 s; 1408 s; 1398 s; 1356 s; 1276 m; 1260 m; 1244 m; 1226 s; 1198 m; 1178 s; 1138 s; 1116 m; 1094 s; 1040 m; 1026 m; 952 m; 930 m; 898 m; 866 s; 820 w; 792 m; 784 m; 758 m; 732 m; 606 m; 580 m; 474 s cm^{-1}.

$C_{52}H_{96}N_2O_{10}Eu_2$ (1213.25): calcd C 51.48, H 7.98, N 2.31; found C 51.58, H 8.05, N 2.40%. IR data: $\tilde{\nu}$ = 2962 s; 2902 s; 2864 s; 2836 m; 2792 m; 1588 s; 1574 s; 1546 s; 1538 s; 1506 s; 1492 s; 1480 s; 1462 s; 1454 s; 1418 s; 1398 s; 1388 s; 1358 s; 1284 m; 1244 s; 1226 s; 1198 m; 1178 s; 1140 s; 1102 m; 1072 s; 1034 m; 1024 m; 962 m; 938 m; 868 s; 820 w; 792 m; 780 w; 756 m; 734 m; 722 w; 668 w; 602 m; 572 w; 476 s cm^{-1}. LDI-TOF MS (EI$^+$): 1029, $[Eu_2(thd)_3((H_3C)_3CCOCH)(O(CH_2)_2NMe_2)]^+$ (10%); 1124, $[Eu_2(thd)_4(O(CH_2)_2NMe_2)]^+$ (30%); 1219, $[Eu_2(thd)_5]^+$ (100%).

$C_{52}H_{96}N_2O_{10}Gd_2$ (1223.83): calcd C 51.03, H 7.91, N 2.29; found C 50.96, H 7.98, N 2.35%. IR data: $\tilde{\nu}$ = 2960 s; 2900 s; 2864 m; 2836 m; 2792 w; 1590 s; 1574 s; 1546 s; 1538 s; 1506 s; 1492 s; 1480 s; 1458 s; 1418 s; 1398 s; 1388 s; 1358 s; 1284 m; 1244 s; 1226 s; 1198 m; 1178 s; 1140 s; 1102 m; 1094 w; 1072 s; 1034 m; 1024 m; 962 m; 938 m; 868 s; 820 w; 792 m; 780 w; 756 m; 734 m; 722 w; 602 m; 574 w; 476 s cm^{-1}.

$C_{52}H_{96}N_2O_{10}Tb_2$ (1227.18): calcd C 50.89, H 7.88, N 2.28; found C 50.50, H 7.85, N 2.15%. IR data: $\tilde{\nu}$ = 2958 s; 2952 s; 2900 m; 2862 m; 2836 w; 2792 w; 1590 s; 1576 s; 1546 s; 1538 s; 1506 s; 1490 s; 1480 s; 1452 s; 1418 s; 1396 s; 1388 s; 1356 s; 1284 m; 1244 m; 1226 m; 1198 m; 1178 m; 1140 m; 1102 w; 1092 w; 1072 m; 1034 w; 1024 w; 962 w; 938 w; 868 m; 820 w; 792 m; 780 w; 756 w; 734 w; 604 w; 576 w; 476 m cm^{-1}.

$C_{52}H_{96}N_2O_{10}Tm_2$ (1247.19): calcd C 50.08, H 7.76, N 2.25; found C 49.71, H 7.80, N 2.08%. IR data: $\tilde{\nu}$ = 2978 s; 2962 s; 2924 s; 2900 m; 2860 m; 2834 w; 2790 w; 1594 s; 1574 s; 1548 m; 1538 m; 1504 s; 1490 s; 1480 s; 1454 s; 1426 s; 1408 s; 1398 s; 1356 s; 1276 m; 1244 m; 1226 m; 1198 w; 1180 m; 1140 m; 1094 m; 1072 m; 1026 w; 954 w; 930 w; 868 m; 820 w; 792 m; 784 w; 758 w; 730 w; 606 w; 582 w; 476 m cm^{-1}.

$C_{52}H_{96}N_2O_{10}Lu_2$ (1259.26): calcd C 49.60, H 7.68, N 2.22; found C 49.35, H 7.68, N 2.28%. IR data: $\tilde{\nu}$ = 2980 s; 2956 s; 2922 s; 2902 m; 2862 m; 2834 m; 2790 w; 1596 s; 1576 s; 1548 m; 1538 m; 1504 s; 1490 s; 1482 s; 1452 s; 1426 s; 1410 s; 1398 s; 1356 s; 1276 m; 1244 m; 1226 m; 1198 w; 1180 m; 1140 m; 1096 m; 1072 m; 1024 w; 954 w; 930 w; 900 w; 868 m; 820 w; 792 m; 784 w; 758 w; 732 w; 606 w; 584 w; 478 m cm^{-1}.

Preparation of the doped by Eu^{III} (or Tb^{III}) Lu^{III} complexes. A toluene solution of Lu^{III} and Eu^{III} (or Tb^{III}) complexes in calculated amounts (0.01, 0.05, 0.1%) were mixed under stirring. The resulting mixtures were left for crystallization until full evaporation of the solvent and then the solid products were thoroughly grinded in a mortar and dried in vacuum.

Data Collection and Structural Refinement. Diffraction data were collected on a Bruker SMART charge-coupled device (CCD) diffractometer at room-temperature routinely to 2θ = 56°. The data was then limited intentionally by introducing a high-angle cutoff for the ranges, where only a minor fraction of all reflections was really observed. The SAINT PLUS and the SHELXTL-NT program packages were used for data reduction and computations.[15] Empirical absorption correction was applied using the Bruker SADABS program package. The positions of all non-hydrogen atoms were refined anisotropically by full-matrix least-squares techniques. In the crystal structure of $[Tb_2(hfa)_6(O(CH_2)_2NHMe_2)_2]\cdot C_7H_8$, a noticeable rotational disorder through elongated thermal ellipsoids for the F atoms of the CF_3 groups in the hfa^- ligand was observed. The latter in combination with low reflectivity at higher angles did not permit to resolve the geometric disorder in the crystal structure of hfa^--containing complex. The hydrogen atoms, except for H1N and H2N in $[Tb_2(hfa)_6(O(CH_2)_2NHMe_2)_2]\cdot C_7H_8$, which were found in differential Fourier syntheses and refined isotropically, were included in calculated positions and refined in a riding mode. Crystallographic data and some details of data collection and structures refinement are listed in Table 1.

Electrochemical Measurements. Cyclic voltammograms were recorded with a BAS CV-100W voltammetric analyzer and a three-electrode system consisting of a stationary Pt disk as working electrode, Pt wire auxiliary electrode, and nonaqueous silver reference electrode (Ag wire in 0.1 M NBu_4PF_6 + 0.01 $AgNO_3$ solution in CH_3CN or THF) in an argon glove box. NBu_4PF_6 (0.1 M in CH_3CN or THF) served as inert electrolyte and the concentration of the complex in solution was 10^{-2} M. The scan rate was 0.1 V·s^{-1}. The voltammograms were analyzed according to the established procedures.[16]

Luminescence Measurements. At 295 K, the luminescence data (spectra, lifetimes) were recorded with a Fluorolog FL3−

22 spectrofluorimeter from Horiba-Jobin-Yvon-Spex. At 77 K, the luminescence spectra were measured using a multichannel spectrometer S2000 (Ocean Optics) with nitrogen laser LGI-21 ($\lambda_{ex} = 337$ nm) as an excitation source, and lifetimes were determined using boxcar averager system (model 162) including gated integrators (model 164) and wide-band preamplifier (model 115) from EG&G Princeton applied research. Lifetimes of the compounds were recorded upon excitation of either the Eu^{III} ($^5D_2$) or Tb^{III} ($^5D_4$) or the organic ligands and monitoring the $^5D_0 \rightarrow {}^7F_2$ or $^5D_4 \rightarrow {}^7F_5$ transitions, respectively. Lifetimes are averages of at least three independent measurements. All luminescence decays proved to be perfect single-exponential functions. Excitation spectra were measured at 295 K with a Fluorolog FL3−22 spectrofluorimeter from Horiba-Jobin-Yvon-Spex upon monitoring the $^5D_0 \rightarrow {}^7F_2$ and $^5D_4 \rightarrow {}^7F_5$ transitions for Eu^{III} and Tb^{III} compounds, respectively. All excitation and luminescence spectra were corrected for the instrumental functions. All measurements were performed on well grinded thick solid samples in special cells.

Quantum yields were determined on solid samples with a Fluorolog FL3−22 spectrofluorimeter from Horiba-Jobin-Yvon-Spex at 295 K, under ligand excitation, according to the absolute method of Wrighton.[17] Each sample was measured several times under slightly different experimental conditions. The estimated error for quantum yields is ±10%.

Diffuse Reflectivity Spectra. UV−vis reflectance spectra for solid samples of Gd^{III} complexes (Figure S1, Supporting Information) were recorded with a Lambda 35 spectrophotometer (Perkin-Elmer).

Refractive Index and Thickness of Thin Films. Thin films of $[Eu_2(hfa)_6(O(CH_2)_2NHMe_2)_2]$ were deposited on quartz substrates by vacuum evaporation ($P \sim 10^{-6}$ Torr, Leybold Heraeus). The refractive index (n) and the thickness of the layer (d) were determined with a Filmetric F20 Thin Film Analyzer. The results are averages of at least three measurements. $[Eu_2(hfa)_6(O(CH_2)_2NHMe_2)_2]$ (thin film): $n = (1.5127 \pm 0.0008)$, $d = (292 \pm 16)$ nm.

Results and Discussion

Synthesis and Characterization. The reaction of *N*,*N*-dimethylaminoethanol with lanthanide(III) hexafluoroacetylacetonates and dipivaloylmethanates in a molar ratio 1:1 in toluene afforded two different types of mixed-ligand complexes depending on the nature of the β-diketone, Hdik. According to previously reported studies[6,18] of similar reactions between $[Cu(hfa)_2]$ and different aminoalcohols, the following scheme can be proposed to discuss the interaction between *N*,*N*-dimethylaminoethanol and $[M(dik)_x(H_2O)_n]$ in toluene (Scheme 1, with $x = 3$ in the case of Ln^{III} ions and 2 for Cu^{II}).

Obviously, the formation of the mixed β-diketonato-alkoxide complexes (type **2**, Scheme 1) is governed by the acidity of Hdik. In principle, the acidity of aliphatic alcohols is much smaller ($pK_a(H_2O) \sim 15$)[19] than the acidity of most β-diketones, for example, $pK_a(H_2O) = 4.4$[20] or 5.3[21] for Hhfa. In the case of $[Cu(hfa)_2]$ in toluene, aminoalcohols such as triethanolamine or *N*,*N*-dimethylethanolamine coordinate in a bidentate fashion and the binding of the N atom causes a weakening of the Cu−O bonds resulting in an increase in the Brønsted basicity of hfa^- oxygen atoms; as a consequence, the ancillary ligand replaces a hfa^- anion and mixed, monomeric or dimeric complexes form.[6] The same authors have also mentioned that the formation of mixed β-diketonato-alkoxide complexes in toluene can be initiated by rising the temperature over the boiling point of Hhfa (63 °C),[20] which is then displaced by evaporation from the

SCHEME 1: Possible Ways of Interaction between $[M(dik)_x(H_2O)_n]$ and *N*,*N*-dimethylaminoethanol in Toluene

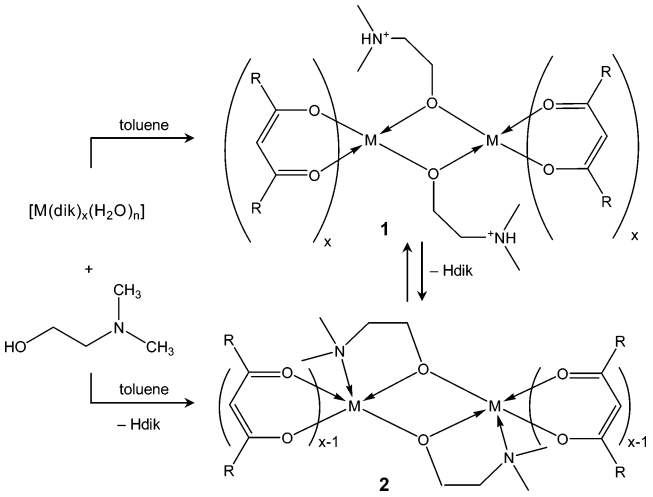

reaction mixture. In our case, interaction between $[Ln(hfa)_3(H_2O)_2]$ and *N*,*N*-dimethylaminoethanol in toluene results in the formation of $[Ln_2(hfa)_6(\mu_2\text{-}O(CH_2)_2NHMe_2)_2]$ (type **1**, Scheme 1) only and a prolonged reflux (>12 h) of the reaction mixture does not lead to the isolation of mixed hexafluoroacetylacetonato-alkoxide complexes (type **2**). Because Ln^{III} ions are harder Lewis acids than Cu^{II}, the formation of mixed β-diketonato-alkoxide complexes is more difficult and requires special conditions to shift the equilibrium (Scheme 1) toward the formation of type **2** products, for instance, a β-diketone having comparable acidity as *N*,*N*-dimethylaminoethanol. This is indeed the case for the reaction of $[Ln(thd)_3]$ ($pK_{a,Hthd}(H_2O) = 11.6 - 14.4$)[22] with *N*,*N*-dimethylaminoethanol which results in the displacement of one of the thd^- ligands; the proton of the aminoalcohol is transferred onto one of the β-diketonato moiety which is then eliminated under the form of Hthd; the overall process yields exclusively the mixed β-diketonato-alkoxide complexes, $[Ln(thd)_2(\mu_2,\eta^2\text{-}O(CH_2)_2NMe_2)]_2$.

Infrared spectra of $[Ln_2(hfa)_6(O(CH_2)_2NHMe_2)_2]$ and $[Ln(thd)_2(O(CH_2)_2NMe_2)]_2$ are similar for all the studied lanthanide ions. They display the typical ν(C═O) and ν(C═C) modes in the range 1700−1500 cm^{-1}, as observed for other lanthanide β-diketonates.[23] For $[Ln_2(hfa)_6(O(CH_2)_2NHMe_2)_2]$, typical C−F vibrations are observed in the range 1300−1100 cm^{-1} and bands of C−H vibrations of *N*,*N*-dimethylaminoethanol ligand can be seen at 3000−2900 cm^{-1}, and for $[Ln(thd)_2(O(CH_2)_2NMe_2)]_2$ the latter are overlapped with strong C−H vibrations characteristic for thd^- at 3000−2800 cm^{-1}. Evidence for the formulation of the compounds with respect to the coordination mode of the aminoalcohol is seen in the range 3500−3200 cm^{-1} in which O−H and N−H vibrations occur for $[Ln_2(hfa)_6(O(CH_2)_2NHMe_2)_2]$ although they are absent from the spectra of $[Ln(thd)_2(O(CH_2)_2NMe_2)]_2$.

In view of the "soft" desorption/ionization of the sample provided by LDI-TOF mass spectrometry, which avoids destructive fragmentation of the compounds,[24] we have resorted to this technique to ascertain the presence of dimeric species in our samples and have chosen the Eu^{III} samples for their typical isotopic distribution. Interpretation of these spectra was made using the general rules of fragmentation of lanthanide β-diketonates described for other mass-spectrometry techniques.[25] The two dimeric complexes present different patterns of fragmentation. The spectrum of $[Eu_2(hfa)_6(O(CH_2)_2NHMe_2)_2]$ is relatively complicated by the strong ability of metal hexafluoroacetyl-

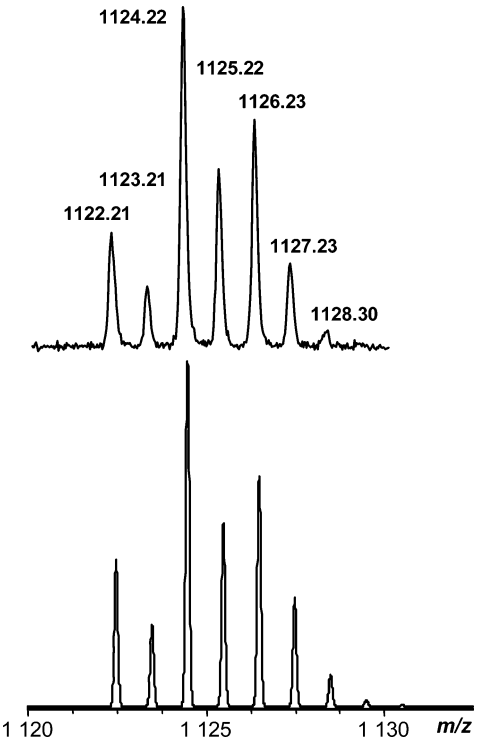

Figure 1. (top) Isotopic distribution of $[Eu_2(thd)_4(O(CH_2)_2NMe_2)]^+$ peak in LDI-TOF mass spectrum of $[Eu(thd)_2(O(CH_2)_2NMe_2)]_2$. (bottom) Calculated isotopic distribution in this species using IsoPro 3.0 MS/MS software.

acetonates to form intermolecular F···F contacts resulting in oligomeric fragments, as well as by the easy splitting of CF_3 fragments and possibility of migration of the F atoms. The three main peaks at $m/e = 959$, 1053, and 1148 are assigned to dimeric fragments with two bridging *N,N*-dimethylaminoethanol ligands; additional peaks correspond to monomeric and trimeric fragments. The spectrum of $[Eu(thd)_2(O(CH_2)_2NMe_2)]_2$ is simpler and displays only three peaks assigned to dimeric fragments, $[Eu_2(thd)_5]^+$ ($m/e = 1219$, 100%), $[Eu_2(thd)_4(O(CH_2)_2NMe_2)]^+$ (1124, 30%), and another entity with a partially fragmented β-diketonato moiety. The isotopic patterns for all the species in mass spectra closely resemble calculated ones as is exemplified in Figure 1 for $[Eu_2(thd)_4(O(CH_2)_2NMe_2)]^+$.

Crystal and Molecular Structures. Single crystals of the Tb^{III} derivatives were isolated from toluene solutions and analyzed by X-ray diffraction. Both compounds crystallize in monoclinic space groups (Table 1) and their crystal structures consist in dimeric units $[Tb_2(hfa)_6(O(CH_2)_2NHMe_2)_2]$ (Figure 2) and $[Tb(thd)_2(O(CH_2)_2NMe_2)]_2$ (Figure 3). Selected bond lengths and angles are summarized in Tables 2 and 3.

In $[Tb_2(hfa)_6(O(CH_2)_2NHMe_2)_2]$, the two Tb^{III} centers are bridged by two oxygen atoms from the two zwitterionic *N,N*-dimethylaminoethanol ($^+HN(Me)_2(CH_2)_2O^-$) ligands. The Tb1···Tb2 separation is 3.684(1) Å while the mean deviation from the plane of the bridging Tb1OOTb2 core is 0.173 Å. Within a noncentrosymmetric dimer, each Tb^{III} ion is also bound to six oxygen atoms from three bidentate chelating hexafluoroacetylacetonato groups resulting in an eight-coordinate environment. The $Tb-O_{hfa}$ distances range from 2.344(7) to 2.492(7) Å for Tb1 and from 2.363(7) to 2.430(7) Å for Tb2 with an overall mean value of 2.39 Å in conformity with the suggestion that coordination of aminoalcohol induces a noticeable lengthening and weakening of some M−O bonds.[6] As a comparison, the mean $Tb-O_{hfa}$ distance is 2.35 Å for $[Tb(hfa)_3(H_2O)_2]$ in

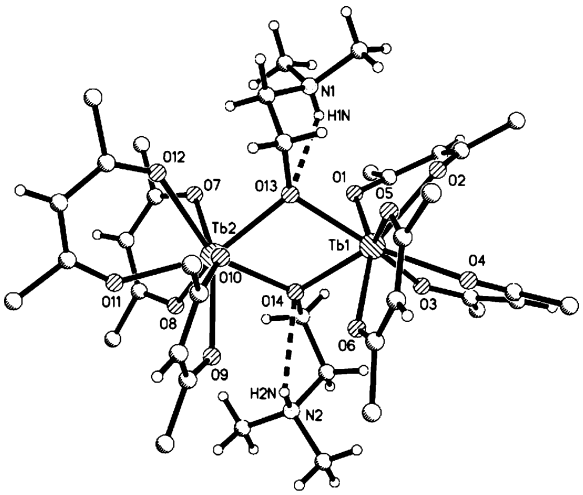

Figure 2. Molecular structure of $[Tb_2(hfa)_6(O(CH_2)_2NHMe_2)_2]\cdot C_7H_8$. Fluorine atoms and solvate toluene molecule are omitted for clarity.

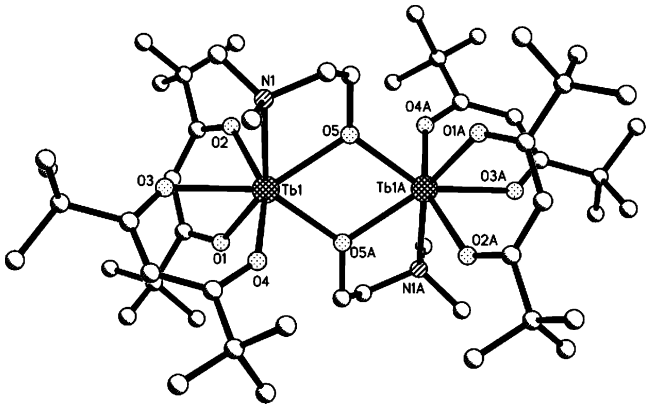

Figure 3. Molecular structure of $[Tb(thd)_2(O(CH_2)_2NMe_2)]_2$. Hydrogen atoms are omitted for clarity.

TABLE 2: Selected Bond Lengths (Å) and Angles (°) in the Crystal Structure of $[Tb_2(hfa)_6(O(CH_2)_2NHMe_2)_2]\cdot C_7H_8$

bond lengths		angles	
Tb1···Tb2	3.684(1)	O2 − Tb1 − O1	68.2(2)
Tb1 − O1	2.492(7)	O3 − Tb1 − O4	70.1(2)
Tb1 − O2	2.360(8)	O5 − Tb1 − O6	72.7(2)
Tb1 − O3	2.344(7)	O7 − Tb2 − O8	70.2(2)
Tb1 − O4	2.435(8)	O10 − Tb2 − O9	70.6(2)
Tb1 − O5	2.362(7)	O11 − Tb2 − O12	68.9(2)
Tb1 − O6	2.372(7)	O13 − Tb1 − O14	71.1(2)
Tb2 − O7	2.374(6)	O14 − Tb2 − O13	70.8(2)
Tb2 − O8	2.395(7)	Tb1 − O13 − Tb2	106.8(2)
Tb2 − O9	2.421(7)	Tb2 − O14 − Tb1	105.8(2)
Tb2 − O10	2.363(7)	N1 − H1N···O13	103.6(6)
Tb2 − O11	2.372(7)	N2 − H2N···O14	114.6(6)
Tb2 − O12	2.430(7)		
Tb1 − O13	2.281(6)		
Tb2 − O13	2.307(6)		
Tb1 − O14	2.314(6)		
Tb2 − O14	2.309(6)		
N1 − H1N···O13/N1···O13	2.47(6)/2.83(1)		
N2 − H2N···O14/N2···O14	2.32(7)/2.86(1)		

$\{[Tb_2(hfa)_4(\mu_2\text{-}O_2CCF_3)_2(H_2O)_4][Tb(hfa)_3(H_2O)_2]_2\cdot H_2O\}$[26] and $[Tb(hfa)_3(TPPO)_2]$,[27] 2.36 Å for $[Tb(hfa)_3(4\text{-cpyNO})]_2$,[28] and 2.38 Å for $[Tb(hfa)_3(diglyme)]$.[29] The average Tb−O bond length in the $Tb_2(\mu\text{-}O)_2$ core (2.30 Å) is shorter than the average distance with the anionic hexafluoroacetylacetonato ligands, which is not typical for dimeric structures with neutral bridging ligands[27,28,30] for which an inverse situation has usually been observed. On the other hand, similar variations in the Ln−O bond lengths have been found in the mixed β-diketonato-

TABLE 3: Selected Bond Lengths (Å) and Angles (°) in the Crystal Structure of $[Tb(thd)_2(O(CH_2)_2NMe_2)]_2$

bond lengths		angles	
Tb1···Tb1A[a]	3.735(2)	O1 − Tb1 − O2	73.5(1)
Tb1 − O1	2.277(4)	O4 − Tb1 − O3	72.3(1)
Tb1 − O2	2.288(3)	O5 − Tb1 − N1	68.2(2)
Tb1 − O3	2.344(4)	O5A − Tb1 − O5	68.6(2)
Tb1 − O4	2.274(4)		
Tb1 − O5	2.268(3)		
Tb1 − O5A	2.256(3)		
Tb1 − N1	2.655(4)		

[a] Symmetry code $1-x, -y, -z$.

alkoxide complexes $[Er(hfa)_2(\mu\text{-}OCH_3)(Q)]_2$ (Q = 2,2′-bipyridine or 1,10-phenanthroline)[31] and $[Pr_2(hfa)_4(bdmap)_2(H_2O)_2\text{-}(THF)_2]$ (bdmap = 1,3-bis(dimethylamino)-2-propoxide).[9] The zwitterionic character of the bridging ($^+HN(Me)_2(CH_2)_2O^-$) ligands is further highlighted by the fact that the proton linked to the nitrogen atom of the alkoxide ligand interacts with the bridging oxygen of the same ligand. This intramolecular hydrogen bond is characterized by distances of 2.84(1) (N1···O13) and 2.86(1) Å (N2···O14), and by angles of 111.5(5) (N1−H1N···O13) and 112.9(5)° (N2−H2N···O14).

The crystal structure of $[Tb(thd)_2(O(CH_2)_2NMe_2)]_2$ (Figure 3) consists in centrosymmetric dimers in which the Tb^{III} centers are bridged by two oxygen atoms from the alkoxide ligand with a Tb1···Tb1A separation of 3.735(2) Å. In addition, each Tb^{III} ion coordinates to four oxygen atoms from two bidentate chelating thd^- ligands and one nitrogen atom from one *N*,*N*-dimethylaminoethoxide thus adopting a seven-coordinate environment. Therefore, *N*,*N*-dimethylaminoethanol acts as anionic ligand with both chelating and bridging modes. Due to the presence of the inversion center, the Tb1OOTb1A core is completely planar. The mean $Tb-O_{thd}$ bond length (2.30 Å) is similar to the one reported for terbium tris(dipivaloylmethanato) complexes with different neutral ancillary ligands.[32] The Tb−O distances within the bridging $Tb_2(\mu\text{-}O)_2$ moiety range from 2.256(3) to 2.268(3) Å, and the average value (2.26 Å) is shorter than the mean $Tb-O_{thd}$ bond length, which is in line with the reported data for mixed β-diketonato-alkoxide complexes.[9,31] The Tb−N distance (2.655(4) Å) is significantly longer than the Tb−O one. This agrees with poorer affinity of the nitrogen atoms to the lanthanide center in comparison with oxygen.[11]

To describe and compare the geometry of the parent lanthanide tris(β-diketonates) with the new mixed-ligand complexes and to evaluate the degree of distortion from ideal geometry, the "shape measure" criterion *S*, suggested by Raymond et al., was estimated as[33]

$$S = \min\sqrt{((1/m)\sum_{i=1}^{m}(\delta_i - \theta_i)^2)} \qquad (1)$$

where *m* is the number of all possible edges, δ_i is the observed dihedral angle (angle between the normal of adjacent faces) along the *i*th edge of the experimental polyhedron δ, and θ_i is the same angle for the corresponding ideal polytopal shape θ. Detailed analysis of the data (Tables 4, S1−S3, Figures S2, S3, Supporting Information) shows that in the crystal structure of $[Tb_2(hfa)_6(O(CH_2)_2NHMe_2)_2]$ both Tb^{III} ions adopt a highly distorted square antiprismatic (SAP) coordination geometry. The square faces of the SAP around Tb1 are formed by the atoms O3, O4, O6, O14 (mean deviation = 0.257 Å) and O1, O2, O5, O13 (0.242 Å), and the ones around Tb2 are delineated by atoms O7, O8, O11, O12 (0.162 Å) and O9, O10, O13, O14 (0.105 Å), the dihedral angles between the corresponding planes being 2.5° and 7.4°, respectively. In comparing the shape measure for $[Tb_2(hfa)_6(O(CH_2)_2NHMe_2)_2]$ and the parent $[Tb(hfa)_3(H_2O)_2]$ β-diketonate,[26] one notes the lower value for the latter thus indicating that the presence of the ancillary ligand is distorting the idealized SAP geometry to a greater extent than water. A similar analysis for $[Tb(thd)_2(O(CH_2)_2NMe_2)]_2$ shows that the coordination polyhedron is closer to a monocapped trigonal prism or monocapped octahedron than to a pentagonal bipyramid, but a precise attribution is not possible in view of the very similar values of $S(C_{2v})$ and $S(C_{3v})$. The lighter lanthanides (La−Gd) form monoclinic dimers with Hthd with space group $P2_1/c$ upon crystallization from *n*-hexane or vapor phase, and the heavier lanthanide tris(dipivaloylmethanates) crystallize as orthorhombic monomers in space group $Pmn2_1$; furthermore, the existence of both types of complexes has been evidenced for Tb^{III} and Dy^{III}.[34−36] Atom coordinates are only available for Pr^{III},[37] Gd^{III},[38] Er^{III},[34] and Lu^{III} [39] tris(dipivaloylmethanates) so that we have used $[Gd_2(thd)_6]$ data for a comparison of the shape measure values with $[Tb(thd)_2\text{-}(O(CH_2)_2NMe_2)]_2$. The coordination polyhedron around the two Gd^{III} ions can be described as monocapped octahedron with a $S(C_{3v})$ value being approximately 1.4-fold smaller than the one for the Tb^{III} ions in $[Tb(thd)_2(O(CH_2)_2NMe_2)]_2$. Consequently, a higher degree of distortion is induced by the presence of the *N*,*N*-dimethylaminoethanol ligand, as in the case of hfa^--containing complexes.

TABLE 4: Comparison of the "Shape Measure" Criteria S[33] (°) for the Crystal Structures of the Novel Mixed-Ligand Complexes and Known β-diketonates

		$[Gd_2(thd)_6]$ [a]	
	$[Tb(thd)_2(O(CH_2)_2NMe_2)]_2$	around Gd1	around Gd2
$S(C_{2v})$ monocapped trigonal prism	8.88	10.50	10.33
$S(C_{3v})$ monocapped octahedron	8.54	6.23	6.00

	$[Tb_2(hfa)_6(O(CH_2)_2NHMe_2)_2]$		
	around Tb1	around Tb2	$[Tb(hfa)_3(H_2O)_2]$[b]
$S(D_{4d})$ square antiprism	12.58	8.44	4.62

[a] From ref 38. [b] From ref 26.

Thermal Analysis and Vacuum Sublimation. The thermal behavior of the new mixed-ligand complexes was examined by means of thermogravimetric analysis under nitrogen atmosphere. The general profile of the weight loss is similar for all the studied lanthanides. As an example, TGA curves are presented for the Tb^{III} derivatives in Figure 4. Weight loss occurs in a single step in the temperature ranges of 180−270 °C and 180−300 °C for $[Tb_2(hfa)_6(O(CH_2)_2NHMe_2)_2]$ and $[Tb(thd)_2(O(CH_2)_2\text{-}NMe_2)]_2$, respectively. The total weight loss for $[Tb_2(hfa)_6\text{-}(O(CH_2)_2NHMe_2)_2]$ (~79%) corresponds to the thermal decomposition of the complex into nonvolatile Tb_4O_7 (~79%) and/or oxyfluoride (~78%). However, under reduced pressure ($\sim 10^{-2}$ Torr), $[Tb_2(hfa)_6(O(CH_2)_2NHMe_2)_2]$ can be quantitatively sublimed at 240 °C. The total weight loss for $[Tb(thd)_2(O(CH_2)_2NMe_2)]_2$ (~86%) is higher than that calculated for the transformation into Tb_4O_7 (~69%). This can be attributed to partial sublimation of the mixed β-diketonato-alkoxide complex even under atmospheric pressure. Indeed, when $[Tb(thd)_2(O(CH_2)_2NMe_2)]_2$ is

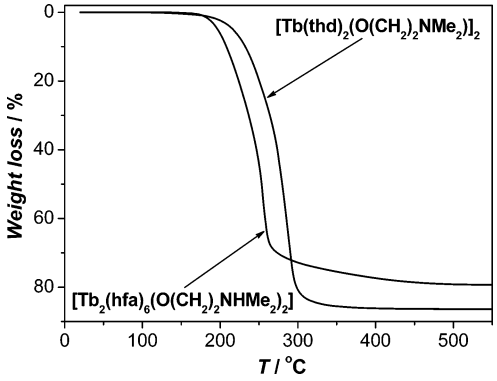

Figure 4. Curves of weight loss of $[Tb_2(hfa)_6(O(CH_2)_2NHMe_2)_2]$ and $[Tb(thd)_2(O(CH_2)_2NMe_2)]_2$ at nitrogen atmosphere.

heated under reduced pressure ($\sim 10^{-2}$ Torr), quantitative sublimation is observed at 220 °C.

Cyclic Voltammetry. Ligand-to-metal charge transfer (LMCT) states are known to play an important role in quenching the Eu^{III} luminescence,[40] but the presence of intense absorption in UV range for lanthanide(III) complexes with organic ligands often prevent the determination of the weaker LMCT absorption expected in the range 300−350 nm. To overcome this limitation, one can resort to cyclic voltammetry, and if the reorganization and solvation energies are assumed to be similar for the Eu^{II} and Eu^{III} complexes the difference ΔE between half peak potentials for ligand oxidation and Eu^{III} reduction will reflect the relative energies of the LMCT states.[16] Taking into account the nature of the organic ligands around the Eu^{III} ion in the reported complexes, the presence of a low-lying LMCT state seems to be most probable in the hfa^--containing β-diketonate. The parent $[Eu(hfa)_3(H_2O)_2]$ hexafluoroacetylacetonate (Figure S4, Supporting Information) displays an irreversible wave for the reduction of Eu^{III} in acetonitrile, which is not the case of $[Eu_2(hfa)_6(O(CH_2)_2NHMe_2)_2]$ because it has a quasi-reversible character. The oxidation waves of the organic ligands are irreversible for both complexes. A rough estimate (in case of irreversible character of reduction/oxidation waves one should operate only with peak potentials) shows that the energy of the LMCT state does not change significantly upon complexation with *N*,*N*-dimethylaminoethanol, and the energy difference between the highest occupied molecular orbital (HOMO) and the lowest unoccupied molecular orbital (LUMO) is around 24 800−25 400 cm^{-1} for the two compounds. Thus, deactivation through the LMCT state is predicted to play a similar and minor role in quenching the luminescence in both the tris(hexafluoroacetylacetonato) complex and in the studied dimer.

On the other hand, the voltammogram of $[Eu_2(hfa)_6(O(CH_2)_2NHMe_2)_2]$ in THF (Figure S5, Supporting Information) features quasi-reversible waves both for the reduction of Eu^{III} and oxidation of the organic ligands. The energy difference between HOMO and LUMO levels is then estimated to be much smaller (16 990 cm^{-1}) than in the case of the solution in acetonitrile. Accordingly, mixing of the LMCT state with 4f functions is expected, as well as a quenching of the Eu^{III} luminescence. The difference with acetonitrile solutions may arise from the basic assumption about solvation and reorganization energies is not valid in our case.

Photophysical Properties. *Ligand-Centered Luminescence in Lu^{III} Complexes.* The luminescence spectra of the Lu^{III} complexes (Figure 5) were measured to determine the energy of the ligand triplet states that may be implied in ligand-to-metal energy transfer processes, because the energy gap between these states and the accepting Ln^{III} states has a significant effect

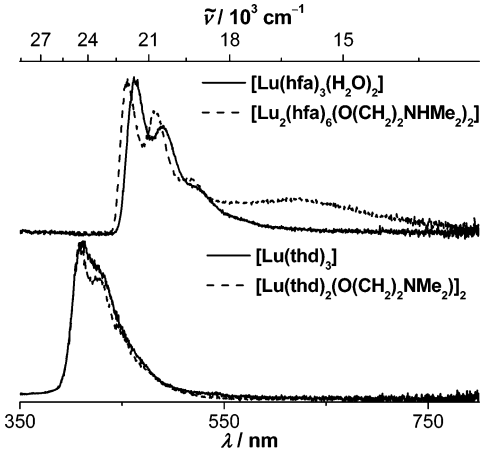

Figure 5. Luminescence spectra of Lu^{III} complexes under excitation at 337 nm; $T = 77$ K.

on energy transfer efficiency and thus on the overall luminescence quantum yield.[41] Because of the filled 4f-shell of Lu^{III} and heavy-atom effect,[42] Lu^{III} complexes provide a mean to probe the ligand excited-state properties in systems structurally very similar to those containing luminescent Ln^{III} ions. The energies of the 0−phonon transitions of the β-diketonato ligands were determined from the luminescence spectra of $[Lu(hfa)_3(H_2O)_2]$ and $[Lu(thd)_3]$, and were at around 21 930 and 24 750 cm^{-1}, respectively, in line with literature data.[28,43] Several attempts were made to synthesize adducts of *N*,*N*-dimethylaminoethanol with Gd^{III} and Lu^{III} nitrates to determine the energy of the triplet state. It was difficult to obtain perfectly reproducible results, but all of the solid products obtained displayed broad emission in the range 350−650 nm with bands centered at 385−405, 450−470, and 595−605 nm (Figure S6, Supporting Information). Thus, the energy of the zero-phonon transition of the triplet state of *N*,*N*-dimethylaminoethanol can be estimated to be $\geq 26\,000$ cm^{-1} ($\lambda \leq 385$ nm).

The Lu^{III} dimer $[Lu_2(hfa)_6(O(CH_2)_2NHMe_2)_2]$ emits in the range 440−800 nm with two maxima at ~456 (21 930 cm^{-1}) and 482 nm (20 750 cm^{-1}), a shoulder at ~518 nm (19 305 cm^{-1}) and a less intense broad band with maximum at ~625 nm (16 000 cm^{-1}). Comparing with the emission spectrum of the parent tris(hexafluoroacetylacetonate) (cf. Figure 5), one notes that the latter is characteristic of the dimer with the other features of the spectrum remaining very similar except for small blue shifts (7−8 nm) and a more pronounced shoulder at ~518 nm. Since the Lu^{III} ion is difficult to reduce or oxidize because of its f^{14} electronic configuration, the band centered at ~625 nm cannot be assigned to metal-to-ligand charge transfer (MLCT) or LMCT transitions; thus, it likely results from intraligand transitions.[44,45] Considering the proposed optimal energy gaps for efficient ligand-to-metal energy transfer[46] the appearance of this long-wavelength band is predicted to have a drastic effect on the sensitization of the Ln^{III} luminescence, increasing the probability of energy back-transfer in the Tb^{III} dimer, although for the Eu^{III} compound it may result in either an increase or a decrease of the metal-centered luminescence.

The luminescence spectra of thd^--containing Lu^{III} complexes present broad bands with maxima at ~408 nm (24 510 cm^{-1}) and vibrational components at ~427 nm (23 420 cm^{-1}), 445 nm (22 470 cm^{-1}) and 470 nm (21 280 cm^{-1}). The envelope of the spectra does not change significantly upon substitution of one of the thd^- by *N*,*N*-dimethylaminoethoxide (Figure 5). In this case and with reference again to the optimal energy gap,[46] it appears that the organic ligands in $[Ln(thd)_2(O(CH_2)_2NMe_2)]_2$

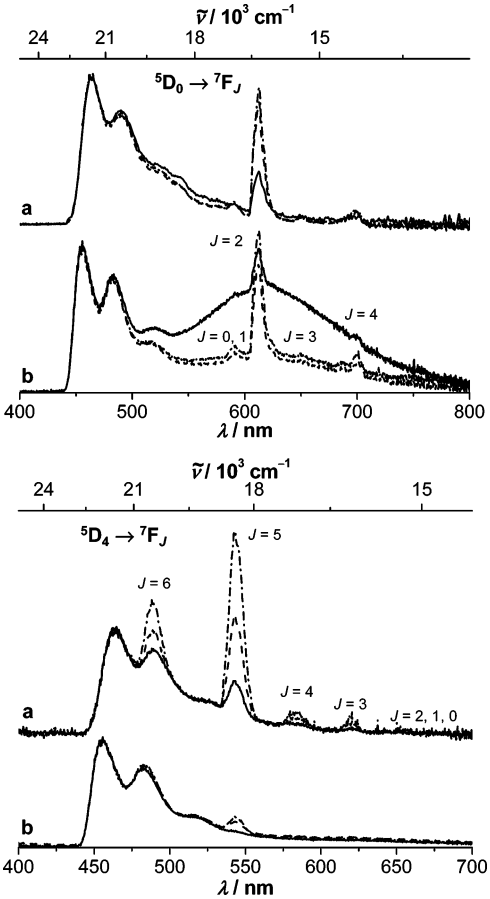

Figure 6. Luminescence spectra of (a) $[Lu(hfa)_3(H_2O)_2]$ and (b) $[Lu_2(hfa)_6(O(CH_2)_2NHMe_2)_2]$ doped by (top) Eu^{III} and (bottom) Tb^{III} (doping rates: — 0.01 mol %, – – 0.05 mol %, – · – · 0.1 mol %) under excitation at 337 nm; $T = 77$ K (normalized on ligand-centered emission).

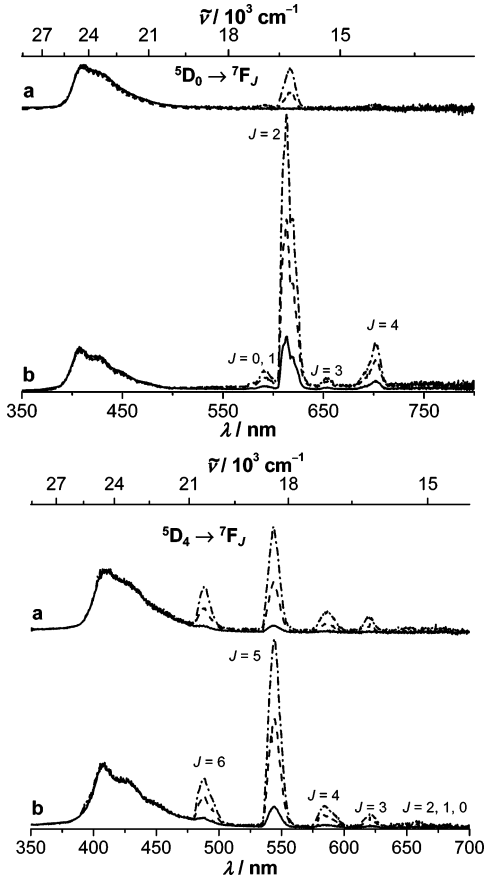

Figure 7. Luminescence spectra of (a) $[Lu(thd)_3]$ and (b) $[Lu(thd)_2(O(CH_2)_2NMe_2)]_2$ doped by (top) Eu^{III} and (bottom) Tb^{III} (doping rates: — 0.01 mol %, – – 0.05 mol %, – · – · 0.1 mol %) under excitation at 337 nm; $T = 77$ K (normalized on ligand-centered emission).

are best suited for the sensitization of Tb^{III} luminescence while the energy gaps are too large for Eu^{III}.

Luminescence of Eu^{III}- and Tb^{III}-Doped Lu^{III} Complexes. To get more information about the role of the ancillary ligand in the energy transfer processes, both Eu^{III}- and Tb^{III}-doped Lu^{III} parent complexes and dimers (doping rates 0.01, 0.05 and 0.1 mol %) were synthesized by cocrystallization and their photoluminescent properties were determined at 77 K. All of these compounds have luminescence spectra containing both the linelike Eu^{III} ($^5D_0 \rightarrow {}^7F_J$) or Tb^{III} ($^5D_4 \rightarrow {}^7F_J$) transitions and the broad-band ligand-centered emission (Figures 6, 7). As expected, the intensity of the metal-centered emission increases with increasing doping rate. The behavior of the ~625 nm feature in the hfa^--containing doped Lu^{III} dimers is very different dependent on the doping ion. For Eu^{III}, the intensity of this feature is maximum for the smaller doping rate and then decreases sharply, and the feature is absent from the spectra of the Tb^{III}-doped samples. A comparison of the intensity ratio of metal-centered to ligand-centered transitions (I_{Ln}/I_L) between equally doped Lu^{III} parent tris(β-diketonates) and mixed-ligand complexes sheds light on the influence of *N*,*N*-dimethylaminoethanol on the efficiency of the energy transfer process (Tables S4, S5, Supporting Information). For 0.1 mol % Eu^{III}-doped hfa^--containing samples, the ratio I_{Ln}/I_L is practically unchanged and for Tb^{III} samples it decreases ~6.6-fold, pointing to a significant negative effect of the ancillary ligand on the metal-centered luminescence (via an increase in back-transfer, vide infra). For thd^--containing complexes, for which the 625 nm feature is absent, the intensity of the metal-centered emission increases more with the doping rate in the dimers compared to the parent tris(β-diketonates). Because of the negligible overlap between ligand- and metal-centered emission, this phenomenon could be characterized by the corresponding integral intensity ratios ($\int_{Ln}/\int_L$) and $\int_{Ln}/\int_{total}$ (Tables S4, S5, Supporting Information). For a doping rate of 0.1 mol %, the increase is about ~2.4-fold in $\int_{Eu}/\int_{total}$ but it is only ~1.2-fold for $\int_{Tb}/\int_{total}$. In addition to this, it is noteworthy that the absolute values of these ratios, 0.29 (parent compound) and 0.69 (dimer) for Eu^{III} and 0.40 and 0.49 for Tb^{III}, are intrinsically large, reflecting the probable existence of extra energy transfer to Eu^{III} or Tb^{III} from the organic ligands coordinated to Lu^{III}. Finally, when the doping rate is increased to 1−2% (data not shown), the ligand-centered luminescence is completely quenched in all the studied monomeric and dimeric compounds, exemplifying a rather efficient $L \rightarrow Ln^{III}$ energy transfer.

Metal-Centered Luminescence. The excitation spectra of the hfa^--containing Eu^{III} and Tb^{III} complexes present broad bands corresponding to the ligand electronic transitions as well as weak and sharp features assigned to f−f transitions (see assignment in Figure 8a). It is noteworthy that the spectrum of the Eu^{III} tris(hexafluoroacetylacetonate) differs markedly from the other excitation spectra in that the feature at around 350−365 nm has a much lower intensity than in the other spectra. In the case of the thd^--containing samples, there is a notable difference between the Eu^{III} and Tb^{III} compounds: the metal-centered f−f transitions largely dominate the spectra of the former, while the Tb^{III} intraconfigurational transitions remain weak compared to the ligand-centered bands (Figure 9a). This is in line with

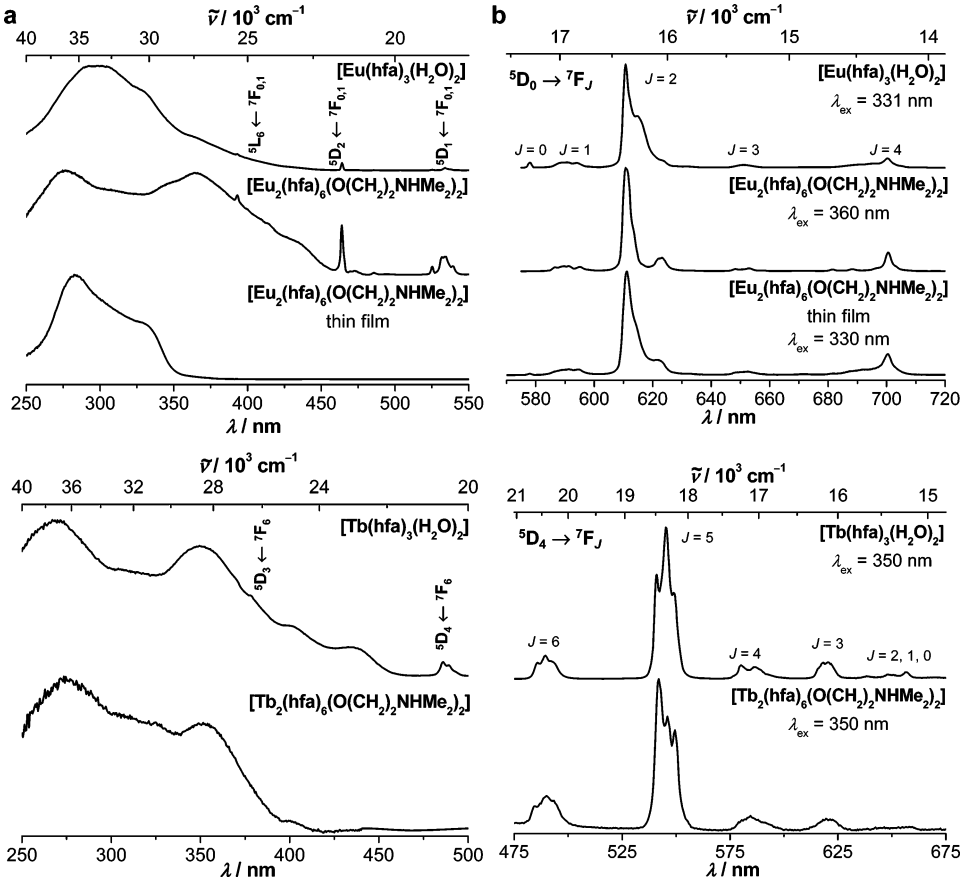

Figure 8. (a) Excitation and (b) emission spectra under ligand excitation of hfa$^-$-containing Eu^{III} and Tb^{III} complexes at 295 K.

the above discussion on the suitability of thd$^-$ for sensitizing the Eu^{III} luminescence. Despite the latter observation, all of the studied Eu^{III} and Tb^{III} complexes display exclusively the narrow metal-centered emission bands upon excitation in the ligand levels (330−380 nm, Figures 8b, 9b). However significant variations in the emission probabilities to the various sublevels, luminescence lifetimes, and quantum yields are observed. The relative integral intensities of the $^5D_0 \rightarrow {}^7F_J$ ($J = 0-4$) and $^5D_4 \rightarrow {}^7F_J$ ($J = 6-0$) transitions are listed in Table 5. It is well documented[47,48] that the luminescent properties of lanthanide ions are very sensitive to variations in the symmetry of the coordination sphere and the polarizability of the coordinated groups. This effect is more sizable for Eu^{III} than for Tb^{III} and results in significant changes in the relative emission intensities, mainly of the hypersensitive transition $^5D_0 \rightarrow {}^7F_2$ and, to a lesser extend, of the $^5D_0 \rightarrow {}^7F_4$ transition. In both mixed-ligand complexes, the integral intensity of the $^5D_0 \rightarrow {}^7F_2$ transition decreases by a factor of ∼1.3 when compared to the corresponding parent Eu^{III} tris(β-diketonates). The influence of the local environment around the metal ions is further demonstrated for the doped Lu^{III} samples of thd$^-$-containing complexes (Figures S7, S8, Tables S6, S7, Supporting Information). For Eu^{III}-containing samples with 0.1 mol % doping rate, the relative integral intensity of the $^5D_0 \rightarrow {}^7F_2$ transition is ∼1.7-fold smaller (∼1.2-fold for $^5D_0 \rightarrow {}^7F_4$) than in the bulk tris(dipivaloylmethanate); in the case of the mixed complex with *N*,*N*-dimethylaminoethoxide, it is however ∼1.3-fold smaller (∼1.5-fold for $^5D_0 \rightarrow {}^7F_4$) compared to the bulk sample. For the Tb^{III} samples, the integral intensities of the $^5D_4 \rightarrow {}^7F_4$ and $^5D_4 \rightarrow {}^7F_3$ transitions are 2.0- and 2.4-fold larger in 0.1% doped [Lu(thd)$_3$] than in the bulk sample, although these values remains practically unchanged for the mixed-ligand complexes. Such significant variations in integral intensities for tris(dipivaloylmethanates) can be attributed to a difference in the crystal structures for light (from La to Gd) and heavy (from Tb to Lu) lanthanides (vide supra), which leads to changing the local environment around central ions. The intensity of the highly forbidden $^5D_0 \rightarrow {}^7F_0$ transition for Eu^{III}-containing samples is also indicative of the symmetry of the metal ion site. It has a relatively large intensity in C_n and C_{nv} symmetries, a geometry easily achieved in [Ln(dik)$_3$(H$_2$O)$_2$] and [Ln(dik)$_3$] (or [Ln$_2$(dik)$_6$]) complexes by distortion from the idealized D_{4d}, respectively D_{3h} (or C_{3v}), geometry. Therefore, the results reported in Table 5 showing that the intensity of the $^5D_0 \rightarrow {}^7F_0$ transition is smaller in the mixed-ligand complexes than in the parent tris(β-diketonates) are consistent with the lowering in symmetry induced by the ancillary ligand, as discussed above (cf. Table 4).

The parameters characterizing the photophysical properties of solid-state samples of the Eu^{III} and Tb^{III} complexes are summarized in Table 6. At room temperature, substitution of the water molecules in Eu^{III} tris(hexafluoroacetylacetonate) by *N*,*N*-dimethylaminoethanol leads to a 4.5-fold increase in the observed luminescence lifetime (τ_{obs}) and to an approximately 22-fold enhancement in absolute overall quantum yield % Q^L_{Eu} as determined upon ligand excitation. Because the intensity of the purely magnetic dipole transition $^5D_0 \rightarrow {}^7F_1$ is independent of the chemical environment around the metal ion, the sensitization efficiency of the organic ligands (η_{sens}) can be estimated using the following equation after calculating the radiative lifetime (τ_{rad}) and the intrinsic quantum yield (Q^{Eu}_{Eu}):[49]

$$\eta_{sens} = \frac{Q^L_{Eu}}{Q^{Eu}_{Eu}}, \quad \text{with } Q^{Eu}_{Eu} = \frac{\tau_{obs}}{\tau_{rad}} \text{ and } \frac{1}{\tau_{rad}} = A_{MD,0} n^3 \left(\frac{I_{tot}}{I_{MD}}\right) \quad (2)$$

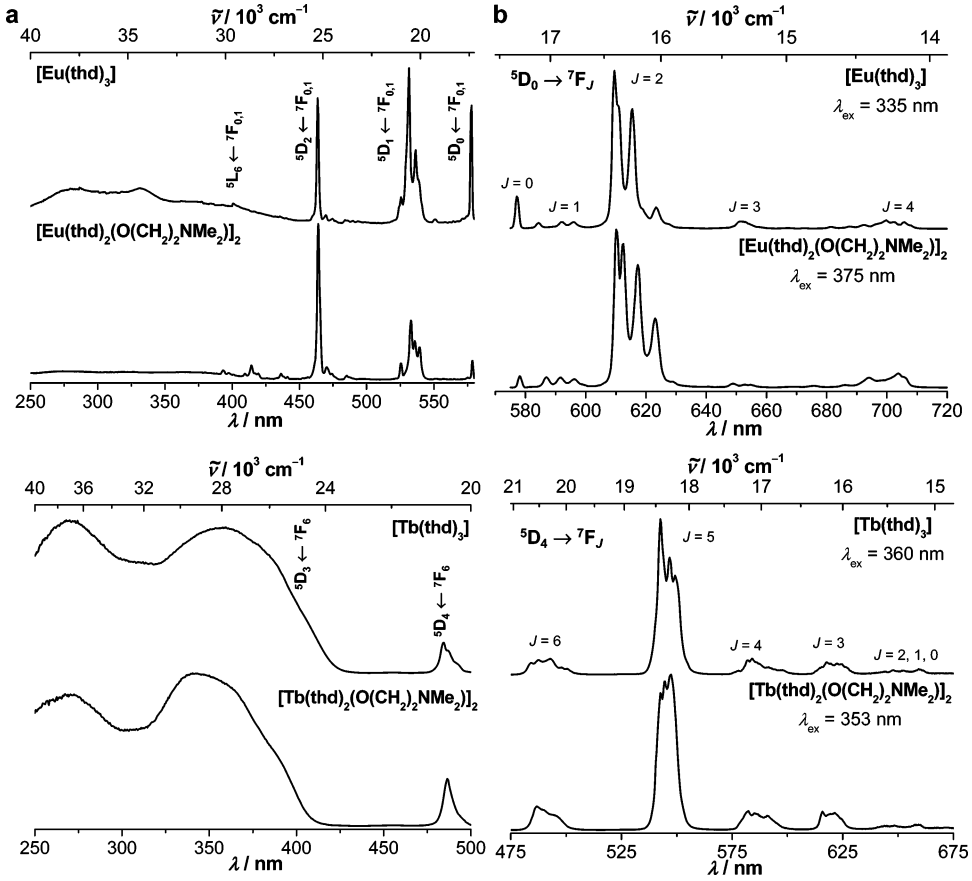

Figure 9. (a) Excitation and (b) emission spectra under ligand excitation of thd$^-$-containing Eu^{III} and Tb^{III} complexes at 295 K.

TABLE 5: Integral Corrected Intensities of the $^5D_0 \rightarrow {}^7F_J$ and $^5D_4 \rightarrow {}^7F_J$ Relative to the $^5D_0 \rightarrow {}^7F_1$ and $^5D_4 \rightarrow {}^7F_5$ Transitions of Eu^{III} and Tb^{III} Complexes, Respectively, upon Ligand Excitation at 295 K

compound	$\int_{0-0}$	$\int_{0-1}$	$\int_{0-2}$	$\int_{0-3}$	$\int_{0-4}$
[Eu(hfa)$_3$(H$_2$O)$_2$][a]	0.17	1.00	14.30	0.38	1.72
[Eu$_2$(hfa)$_6$(O(CH$_2$)$_2$NHMe$_2$)$_2$]	0.01	1.00	10.83	0.41	1.98
[Eu$_2$(hfa)$_6$(O(CH$_2$)$_2$NHMe$_2$)$_2$] thin film	0.04	1.00	11.17	0.37	2.14
[Eu(thd)$_3$]	1.11	1.00	23.27	1.07	2.41
[Eu(thd)$_2$(O(CH$_2$)$_2$NMe$_2$)]$_2$	0.22	1.00	17.52	0.31	2.10

	$\int_{4-6}$	$\int_{4-5}$	$\int_{4-4}$	$\int_{4-3}$	$\int_{4-2,1,0}$
[Tb(hfa)$_3$(H$_2$O)$_2$] [a]	0.22	1.00	0.11	0.08	0.04
[Tb$_2$(hfa)$_6$(O(CH$_2$)$_2$NHMe$_2$)$_2$]	0.24	1.00	0.13	0.10	0.06
[Tb(thd)$_3$]	0.20	1.00	0.11	0.07	0.04
[Tb(thd)$_2$(O(CH$_2$)$_2$NMe$_2$)]$_2$	0.22	1.00	0.14	0.08	0.04

[a] From ref 28.

where $A_{MD,\,0} \equiv 14.65\ s^{-1}$ is the spontaneous emission probability of the magnetic dipole $^5D_0 \rightarrow {}^7F_1$ transition, n is the refractive index, I_{tot} is the total integrated emission of the $^5D_0 \rightarrow {}^7F_J$ transitions, and I_{MD} is the integrated emission of the $^5D_0 \rightarrow {}^7F_1$ transition. Thus, the substantial contribution of *N*,*N*-dimethylaminoethanol ligand to the overall sensitization process of Eu^{III}-centered luminescence in [Eu$_2$(hfa)$_6$(O(CH$_2$)$_2$NHMe$_2$)$_2$] is confirmed by (i) the increase in the intrinsic quantum yield by a factor of 3.7 resulting from removing the quenching effect of the O−H vibrations, and (ii) the substantial enhancement of η_{sens} from 13 to 81% (i.e., 6.2-fold). Other vibrations contribute only faintly to the nonradiative deactivation processes in the mixed-ligand compound, as demonstrated by the constancy (within experimental error) of τ_{obs} between room and liquid nitrogen temperatures; for [Eu(hfa)$_3$(H$_2$O)$_2$], an ∼1.5-fold increase is observed. The much larger increase in η_{sens} compared with % Q_{Eu}^{Eu} is reflecting the contribution of the ancillary ligand to the energy transfer process. In contrast, substitution of water molecules in [Tb(hfa)$_3$(H$_2$O)$_2$] by *N*,*N*-dimethylaminoethanol is detrimental to luminescent properties at room temperature: both the lifetime (too short to be determined) and quantum yield drop dramatically. This can be traced back to the low energy of the ligand-centered states in the dimeric complex allowing efficient back-energy transfer. The latter is confirmed by the Tb($^5D_4$) lifetime increasing to 1.27 ms at 77 K. Because the lifetime for [Tb$_2$(hfa)$_6$(O(CH$_2$)$_2$NHMe$_2$)$_2$] at liquid nitrogen temperature is ∼1.8-fold larger compared to [Tb(hfa)$_3$(H$_2$O)$_2$], an obvious conclusion is that the ancillary ligand reduces vibrational (O−H) quenching but increases back transfer; its influence on the energy transfer step cannot be assessed in absence of data for the intrinsic quantum yield.

The situation is different for thd$^-$-containing complexes. In going from the unsolvated [Ln(thd)$_3$] complexes to the [Ln(thd)$_2$(O(CH$_2$)$_2$NMe$_2$)]$_2$ dimers, a significant increase in τ_{obs} (295 K) is observed for Eu^{III}: from a value too short to be measured up to 0.47 ms, while an 1.5-fold lengthening results for Tb^{III}. At 77 K, lifetimes of the parent tris(dipivaloylmethanates) and dimers are the same within experimental errors for both Eu^{III} (∼0.5 ms) and Tb^{III} (∼0.6 ms), which is in contrast to what is measured at room temperature. In addition, a small (Eu^{III}) or no significant (Tb^{III}) increases are denoted between 295 and 77 K for the mixed-ligand compounds, which is by large not the case for the parent complexes. Interpretation of these data is straightforward in that they again point to less phonon-assisted deactivation processes in the dimeric complexes; in addition, back-energy transfer is minimized for Tb^{III}. A large enhancement (∼8-fold) in the absolute quantum yield

TABLE 6: Observed and Radiative Lifetimes, Intrinsic and Absolute (±10%) Quantum Yields, and Sensitization Efficiencies of Eu^{III} and Tb^{III} Complexes[a]

compound	λ_{em}, nm	τ_{obs}, ms 295 K	τ_{obs}, ms 77 K	τ_{rad}, ms	% Q_{Eu}^{Eu},%	% Q_{Ln}^{L}, %	η_{sens}, %
$[Eu(hfa)_3(H_2O)_2]$ [b]	610.7	0.22 ± 0.01	0.32 ± 0.01	1.13	19	2.6	13 ± 2
$[Eu_2(hfa)_6(O(CH_2)_2NHMe_2)_2]$	611.0	0.99 ± 0.02	1.04 ± 0.02	1.39	71	58	81 ± 12
$[Eu_2(hfa)_6(O(CH_2)_2NHMe_2)_2]$ thin film	611.0	0.85 ± 0.05	*c*	1.39	61	*c*	*c*
$[Eu(thd)_3]$	609.5	*d*	0.50 ± 0.01	*c*	*c*	0.05	*c*
$[Eu(thd)_2(O(CH_2)_2NMe_2)]_2$	610.1	0.48 ± 0.01	0.53 ± 0.01	0.94	51	0.41	0.8 ± 0.1
$[Tb(hfa)_3(H_2O)_2]$ [b]	545.0	0.54 ± 0.03	0.72 ± 0.01	*c*	*c*	27	*c*
$[Tb_2(hfa)_6(O(CH_2)_2NHMe_2)_2]$	542.0	*d*	1.27 ± 0.01	*c*	*c*	0.04	*c*
$[Tb(thd)_3]$	542.6	0.46 ± 0.04	0.64 ± 0.01	*c*	*c*	40	*c*
$[Tb(thd)_2(O(CH_2)_2NMe_2)]_2$	547.1	0.68 ± 0.02	0.62 ± 0.01	*c*	*c*	32	*c*

[a] Unless otherwise stated, all photophysical data are listed for 295 K; τ_{rad}, % Q_{Eu}^{Eu}, η_{sens} were calculated under the assumption that $n = 1.5127$ for $[Eu_2(hfa)_6(O(CH_2)_2NHMe_2)_2]$ and $n = 1.51$ for the other Eu^{III} complexes. [b] From ref 28. [c] Not determined. [d] Not measurable ($<5 \times 10^{-4}$ ms).

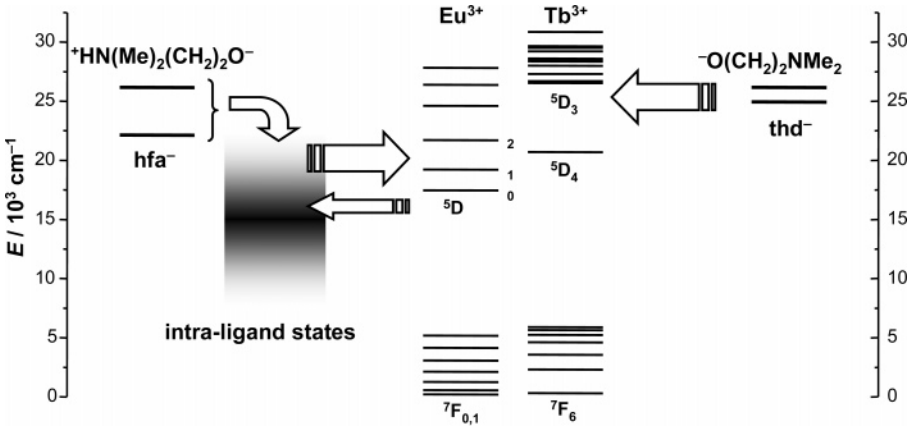

Figure 10. Simplified energy level diagram for (left) $[Lu_2(hfa)_6(O(CH_2)_2NHMe_2)_2]$ and (right) $[Lu(thd)_2(O(CH_2)_2NMe_2)]_2$ and Tb^{III} and Eu^{III} ions.

of the Eu^{III} mixed-ligand complex is observed over the parent tris(dipivaloylmethanate), but its value remains largely under 1%; for this compound, although the value of intrinsic quantum yield is equal to ~51%, the sensitization efficiency is quite low (0.8%).[50] For Tb^{III}, the absolute quantum yield decreases by about 20% in going from the parent tris(dipivaloylmethanates) to the dimeric compounds, while the lifetime increases 1.5-fold. This reflects a combination of minimizing phonon-assisted quenching and diminishing the ligand-to-metal energy transfer efficiency.

Luminescence Properties of $[Eu_2(hfa)_6(O(CH_2)_2NHMe_2)_2]$ Thin Films. Thin films of the most luminescent compound studied, $[Eu_2(hfa)_6(O(CH_2)_2NHMe_2)_2]$, have been obtained by vacuum sublimation at 10^{-6} Torr. Their average thickness was close to 300 nm, and their excitation and emission spectra are reported in Figures 8a and 8b, respectively. The long wavelength feature extending from 358 to ~460 nm in the excitation spectrum of the bulk compound disappears for the thin film sample. The excitation spectrum of the latter displays a clean cutoff at around 350 nm and is in excellent correspondence with the reflectance spectrum of the corresponding Gd^{III} mixed-ligand complex (Figure S1, Supporting Information). This may be related to intermolecular interactions taking place in the bulk sample, which are minimized (or absent) in the thin film. On the other hand, the photoluminescence spectra of the thin film and the bulk sample are very similar (cf. Figure 8b, Tables 5 and 6). The integrated intensities of the $^5D_0 \rightarrow {}^7F_{2,4}$ transitions are slightly larger for the thin film, and the observed luminescence lifetimes at room temperature and intrinsic quantum yield are smaller by about 15%. As a consequence, it is anticipated that the overall quantum yield (not measured) will also be somewhat smaller than for the bulk sample.

Conclusions

This study has demonstrated that the coordination mode of *N*,*N*-dimethylaminoethanol in mixed-ligand lanthanide β-diketonates depends on the nature of the reacting complex, $[Ln(hfa)_3(H_2O)_2]$, or $[Ln(thd)_3]$. Accordingly, two types of dimeric complexes can be obtained: $[Ln_2(hfa)_6(O(CH_2)_2NHMe_2)_2]$ in which *N*,*N*-dimethylaminoethanol acts as bridging ancillary zwitterionic ligand and $[Ln(thd)_2(O(CH_2)_2NMe_2)]_2$ in which it operates as a bridging-chelating anionic ligand. The insertion of *N*,*N*-dimethylaminoethanol in the β-diketonate structures has several consequences on the photophysical properties of the resulting edifices. First, phonon-assisted nonradiative deactivation processes are minimized, especially when the ancillary ligand is replacing water molecules in $[Ln(hfa)_3(H_2O)_2]$; for Ln = Eu^{III}, this leads to a huge enhancement in observed lifetime (from ~0.2 to ~1.0 ms). Assuming that the increase in τ_{obs} arises solely from the removal of the water molecules from the inner coordination sphere, one calculates from the data reported in Table 6 a contribution to the nonradiative rate constant of 505 s^{-1} per water molecule, about half the value found for the aquo-ion.[51] Substitution of one of the thd^- ligands in $[Ln(thd)_3]$ has much less influence, as expected, and similar effects are anticipated for Tb^{III} and Eu^{III} complexes. Second, the ancillary ligand introduces new electronic states, the energy of which depends on its form (zwitterionic or anionic). Thus, a combination of $^+HN(Me)_2(CH_2)_2O^-$ and hfa^- in studied dimeric complexes leads to formation of low-lying energy states that influences both the ligand-to-metal and metal-to-ligand energy transfer processes (Figure 10). With respect to these electronic effects, the consequences differ largely for Eu^{III} compared to Tb^{III}. For samples containing the former ion, luminescence properties are considerably enhanced: in the

hfa^--containing dimer, not only are the nonradiative processes minimized, but in addition the efficiency of the ligand-to-metal energy transfer is improved. This results in a highly luminescent compound with a quantum yield of 58% in the solid state, and an overall sensitization efficiency of ~80%. On the other hand, thd^- has no adequate electronic level for an efficient energy transfer onto Eu^{III}, so that despite the large improvement in quantum yield brought by the insertion of the ancillary ligand (8.2-fold increase in Q^L_{Eu} over the parent tris(β-diketonate)), the resulting complex is poorly emissive. For Tb^{III}, coordination of the ancillary ligand has a negative influence in both studied systems: in the hfa^--containing dimer, back transfer is increased substantially, which more than offsets the advantage of decreasing vibronic-based deactivation and the quantum yield drops by a factor of about 670; the situation is better for the thd^--containing dimeric complex, although the latter is less luminescent than the un-solvated tris(β-diketonate).

As a conclusion, *N*,*N*-dimethylaminoethanol is found to be a simple and an interesting ligand that allows one to tune the metal-centered luminescent properties in lanthanide tris(β-diketonates), generating drastic effects. In addition, the dimeric lanthanide(III) complexes reported are thermally stable, which opens the way to production of highly luminescent thin films, as demonstrated with $[Eu_2(hfa)_6(O(CH_2)_2NHMe_2)_2]$, which is certainly an outstanding candidate for the design of red-emitting electroluminescent materials.

Acknowledgment. We thank Dr. Vladislav V. Lobodin (Organic Chemistry Division, Lomonosov Moscow State University, Moscow) for measuring the LDI-TOF mass spectra, Mr. Andrei A. Vaschenko (Lebedev Physical Institute of Russian Academy of Sciences, Moscow) for his assistance in obtaining the thin films, and the Russian Foundation for Basic Research (Grants 05-03-33090-a, 07-02-00495-a) for financial support.

Supporting Information Available: Crystallographic data in CIF format, figures with comparison of coordination polyhedra around central ions for parent and novel dimeric complexes, cyclic voltammograms, luminescence spectra of Eu^{III} and Tb^{III} complexes and doped by those ions Lu^{III} complexes at 77 K, reflectance spectra; tables with angles and shape measure values and analysis of integral intensities and photophysical data of doped Lu^{III} complexes. This material is available free of charge via the Internet at http://pubs.acs.org.

References and Notes

(1) Binnemans, K. In *Handbook on the Physics and Chemistry of Rare Earths*; Gschneidner, K. A., Jr., Bünzli, J.-C. G., Pecharsky, V. K., Eds.; Elsevier: Amsterdam, 2005; Vol. 35, Chapter 225.

(2) (a) Raber, D. J. *Lanthanide Shift Reagents in Stereochemical Analysis*; Morril, T. C., Eds.; VCH: New York, 1986. (b) Peters, J. A.; Huskens, J.; Raber, D. J. *Prog. Nucl. Magn. Reson. Spectrosc.* **1996**, *28*, 283−350. (c) Forsberg, J. H. In *Handbook on the Physics and Chemistry of Rare Earths*; Gschneidner, K. A., Jr., Eyring L., Eds.; Elsevier: Amsterdam ,1996; Vol. 23, Chapter 153.

(3) (a) Kobayashi, S.; Sugiura, M.; Kitagawa, H.; Lam, W. W. L. *Chem. Rev.* **2002**, *102*, 2227−2302. (b) Imamoto, T. *Lanthanides in Organic Synthesis*; Academic Press: London, 1994.

(4) (a) Shinoda, S.; Miyake, H.; Tsukube, H. In *Handbook on the Physics and Chemistry of Rare Earths*; Gschneidner, K. A., Jr., Bünzli, J.-C. G., Pecharsky, V. K., Eds.; Elsevier: Amsterdam, 2005; Vol. 35, Chapter 226. (b) Tsukube, H.; Shinoda, S. *Chem. Rev.* **2002**, *102*, 2389−2404.

(5) Mehrotra, R. C.; Singh, A.; Tripathi U. M. *Chem. Rev.* **1991**, *91*, 1287−1303.

(6) Pinkas, J.; Huffman, J. C.; Bollinger, J. C.; Streib, W. E.; Baxter, D. V.; Chisholm, M. H.; Caulton, K. G. *Inorg. Chem.* **1997**, *36*, 2930−2937.

(7) Liu, S.; Gelmini, L.; Rettig, S. J.; Thompson, R. C.; Orvig, C. *J. Am. Chem. Soc.* **1992**, *114*, 6081−6087.

(8) Gharia, K. S.; Singh, M.; Mathur, S.; Sankhla, B. S. *Synth. React. Inorg. Met.-Org. Chem.* **1980**, *10*, 403−416.

(9) Wang, S.; Pang, Z.; Smith, K. D. L.; Hua, Y.-S.; Deslippe, C.; Wagner, M. J. *Inorg. Chem.* **1995**, *34*, 908−917.

(10) Sheng, H.; Xu, F.; Yao, Y.; Zhang, Y.; Shen, Q. *Inorg. Chem.* **2007**, *46*, 7722−7724.

(11) Pearson, R. G. *Chemical Hardness: Application from Molecules to Solids*; Wiley-VCH Verlag GmbH: Weinheim, 1997.

(12) (a) Tsukube, H.; Hosokubo, M.; Wada, M.; Shinoda, S.; Tamiaki, H. *J. Chem. Soc., Dalton Trans.* **1999**, 11−12. (b) Tsukube, H.; Hosokubo, M.; Wada, M.; Shinoda, S.; Tamiaki, H. *Inorg. Chem.* **2001**, *40*, 740−745.

(13) Richardson, M. F.; Wagner, W. F.; Dands, D. E. *J. Inorg. Nucl. Chem.* **1968**, *30*, 1275−1289.

(14) Eisentraut, K. J.; Sievers, R. J. *J. Am. Chem. Soc.* **1965**, *87*, 5254−5256.

(15) Sheldrick, G. M. *SHELXTL-NT, Reference Manual*; Bruker AXS: University of Göttingen, Germany, 1998.

(16) (a) Dodsworth, E. S.; Lever, A. B. P. *Chem. Phys. Lett.* **1986**, *124*, 152−158. (b) Lee, Y.-Z.; Chen, X.; Chen, S.-A.; Wei, P.-K.; Fann, W.-S. *J. Am. Chem. Soc.* **2001**, *123*, 2296−2307.

(17) (a) Wrighton, M. S.; Ginley, D. S.; Morse, D. L. *J. Phys. Chem.* **1974**, *78*, 2229−2233. (b) de Mello, J. C.; Wittmann, H. F.; Friend, R. H. *Adv. Mater.* **1997**, *9*, 230−232. (c) Greenham, N. C.; Samule, I. D. W.; Hayes, G. R.; Philips, R. T.; Kessener, Y. A. R. R.; Moratti, S. C.; Holmes, A. B.; Friend, R. H. *Chem. Phys. Lett.* **1995**, *241*, 89−96.

(18) Billodeaux, D. R.; Cygan, Z. T.; Maverick, A. W.; Fronczek, F. R. *J. Chem. Cryst.* **1999**, *29*, 901−906.

(19) Rochester C. H. In *The Chemistry of the Hydroxyl Group*; Patai S., Ed.; J. Wiley & Sons: New York, 1971; Part 1, p 369.

(20) (a) Koshimura, H.; Saito, J.; Okubo, T. *Bull. Chem. Soc. Jpn.* **1973**, *46*, 632−634. (b) Fujinaga, T.; Kuwamato, T.; Kimoto, T. *Talanta* **1976**, *23*, 753. (c) Butts, W. C.; Banks, C. V. *Anal. Chem.* **1970**, *42* (*1*), 133−136.

(21) Reutov, O. A.; Beletskaya, I. P.; Butin, K. P. *CH-acids*; Pergamon Press: New York, 1978; p 192.

(22) (a) Komarov, V. A. *Zh. Anal. Khim.* **1976**, *131*, 366−378. (b) Eisentraut, K. J.; Sievers, R. E. *J. Inorg. Nucl. Chem.* **1967**, *29*, 1931−1936.

(23) Nakanishi, K. *IR Spectroscopy and Structure of Organic Compounds*; Mir: Moscow, 1965 (in Russian).

(24) Lebedev, A. T. *Mass-spectrometry in Organic Chemistry*; Binom, Laboratoriia Znanii: Moscow, 2003 (in Russian).

(25) Gerbeleu, N. V.; Indrichan, K. M. *Mass-spectrometry of Coordination Compounds*; Shtiintca: Kishinev, Russia, 1984 (in Russian).

(26) Drake, S. R.; Lyons, A.; Otway, D. J.; Williams, D. J. *Inorg. Chem.* **1994**, *33*, 1230−1233.

(27) Petrov, V. A.; Marshall, W. J.; Grushin, V. V. *Chem. Comm.* **2002**, 520−521.

(28) Eliseeva, S. V.; Ryazanov, M.; Gumy, F.; Troyanov, S. I.; Bünzli, J.-C. G.; Kuzmina, N. P. *Eur. J. Inorg. Chem.* **2006**, 4809−4820.

(29) Evans, W. J.; Giarikos, D. G.; Johnston, M. A.; Greci, M. A.; Ziller, J. W. *J. Chem. Soc., Dalton Trans.* **2002**, 520−526.

(30) Ma, S.-L.; Zhu, W.-X.; Huang, G.-H.; Yuan, D.-Q.; Yan, X. *J. Mol. Struct.* **2003**, *646*, 89−94.

(31) van Staveren, D. R.; Haasnoot, J. G.; Maire Manotti Lanfredi, A.; Menzer, S.; Nieuwenhuizen, P. J.; Spek, A. L.; Ugozzoli, F.; Reesijk, J. *Inorg. Chim. Acta* **2000**, *307*, 81−87.

(32) (a) Clegg, W.; Sage, I.; Oswald, I.; Brough, P.; Bourhill, G. *Acta Crystallogr., Sect. C* **2000**, C*56*, 1323−1325. (b) Holz, R. C.; Thompson, L. C. *Inorg. Chem.* **1993**, *32*, 5251−5256. (c) Drake, S. R.; Lyons, A.; Otway, D. J.; Slawin, A. M. Z.; Williams, D. J. *J. Chem. Soc., Dalton Trans.* **1993**, 2379−2386.

(33) Xu, J.; Radkov, E.; Ziegler, M.; Raymond, K. N. *Inorg. Chem.* **2000**, *39*, 4156−4164.

(34) de Villiers, J. P. R.; Boeyens, J. C. A. *Acta Crystallogr., Sect. B* **1972**, *B28*, 2335−2340.

(35) Martynenko, L. I.; Kuzmina, N. P.; Grigoriev, A. N. *Russ. J. Inorg. Chem.* **1998**, *43*, 1038−1046 (Zh. Neorg. Khim. **1998**, *43*, 1131−1140).

(36) Amano, R.; Sato, A.; Suzuki, S. *Chem. Lett.* **1980**, 537−540.

(37) Erasmus, C. S.; Boeyens, J. C. A. *Acta Crystallogr., Sect. B* **1970**, B*26*, 1843−1854.

(38) Baxter, I.; Drake, S. R.; Hursthouse, M. B.; Abdul Malik, K. M.; McAleese, J.; Otway, D. J.; Plakatouras, J. C. *Inorg. Chem.* **1995**, *34*, 1384−1394.

(39) Onuma, S.; Inoue, H.; Shibata, S. *Bull. Chem. Soc. Jpn.* **1976**, *49*, 644−647.

(40) (a) Petoud, S.; Bünzli, J.-C. G.; Glanzman, T.; Piguet, C.; Xiang, Q.; Thummel, R. P. *J. Lumin.* **1999**, *82*, 69−79. (b) Gonçalves e Silva, F. R.; Longo, R.; Malta, O. L.; Piguet, C.; Bünzli, J.-C. G. *Phys. Chem. Chem.*

Phys. **2000**, *2*, 5400−5403. (c) Faustino, W. M.; Malta, O. L.; de Sá, G. F.*J. Chem. Phys.* **2005**, *122*, 054109−10. (d) Charbonnière, L. J.; Balsiger, C.; Schenk, K. J.; Bünzli, J.-C. G. *J. Chem. Soc., Dalton Trans.* **1998**, 505−510.

(41) (a) Filipescu, N.; Sager, W. F.; Serafin, F. A. *J. Phys. Chem.* **1964**, *68*, 3324−2246. (b) Sato, S.; Wada, M. *Bull. Chem. Soc. Jpn.* **1970**, *43*, 1955−1962.

(42) (a) Tobita, S.; Arakawa, M.; Tanaka, I. *J. Phys. Chem.* **1985**, *89*, 5649−5654. (b) Tobita, S.; Arakawa, M.; Tanaka, I. *J. Phys. Chem.* **1984**, *88*, 2697−2702.

(43) Voloshin, A. I.; Shavaleev, N. M.; Kazakov, V. P. *J. Lumin.* **2001**, *93*, 199−204.

(44) Wen, L.; Li, Y.; Lu, Z.; Lin, J.; Duan, C.; Meng, Q. *Cryst. Growth Des.* **2006**, *6*, 530−537.

(45) Mahata, P.; Ramya, K. V.; Natarajan, S. *Dalton Trans.* **2007**, 4017−4026.

(46) Bünzli, J.-C. G. In *Spectroscopic Properties of Rare-Earths in Optical Materials*; Liu, G., Jacquier B., Eds.; Springer-Verlag: Berlin, 2005; Chapter 11.

(47) Bünzli, J.-C. G. In *Lanthanide Probes in Life, Chemical and Earth Sciences. Theory and Practice*; Bünzli, J.-C. G., Choppin, G. R., Eds.; Elsevier: Amsterdam, 1989; Chapter 7.

(48) Judd, B. R. *J. Chem. Phys.* **1979**, *70*, 4830−4833.

(49) (a) Chauvin, A.-S.; Gumy, F.; Imbert, D.; Bünzli, J.-C. G. *Spectrosc. Lett.* **2004**, *37*, 517−532. (b) Chauvin, A.-S.; Gumy, F.; Imbert, D.; Bünzli, J.-C. G. *Spectrosc. Lett.* **2007**, *40*, 193.

(50) Estimates of % Q_{Eu}^{Eu} from 77 K spectra for both $[Eu(thd)_3]$ and $[Eu(thd)_2(O(CH_2)_2NMe_2)]_2$ give practically the same value (64 versus 62 %), an additional hint to the poor overall quantum yields for both compound stemming essentially from the energy transfer step.

(51) Haas, Y.; Stein, G. *J. Phys. Chem.* **1971**, *75*, 3668−3677.